Journal of Nano- and Electronic Physics
Vol. 11 No 5, 05026(5pp) (2019)

Журнал нано- та електронної фізики
Том 11 № 5, 05026(5cc) (2019)

Enhanced Optical and Dielectric Properties of PANI/rGO Nanocomposites for Supercapacitor Application

Ajay Kumar Sharma[1,2,*], Praveen Kumar Jain[3], Rishi Vyas[2], Vishal Mathur[4], Vipin Kumar Jain[1]

[1] *Institute of Engineering and Technology, JK Lakshmipat University, Jaipur 302026, India*
[2] *Department of Physics, Swami Keshvanand Institute of Technology, Management & Gramothan, Jaipur 302017, India*
[3] *Department of Electronics and Communication Engineering, Swami Keshvanand Institute of Technology, Management & Gramothan, Jaipur 302017, India*
[4] *Department of Engineering, Sur University College, Oman*

(Received 27 April 2019; revised manuscript received 22 October 2019; published online 25 October 2019)

The conducting polymer nanocomposites have been extensively used due to manifold applications particularly as a novel supercapacitor material. The present work deals with the fabrication of PANI/rGO nanocomposites and investigating their morphological, optical and dielectric properties. The present paper is focused on the synthesis of $(PANI)_{1-x}(rGO)_x$ nanocomposites (x = 0, 0.02, 0.04, 0.06, 0.08) prepared by an in-situ chemical oxidation polymerization of aniline using ammonium peroxide sulfate (APS) as an oxidant in presence of colloidal reduced graphene oxide (rGO) nanoparticles at 0-5 °C in air to improve optical and dielectric constants of PANI for supercapacitor applications. rGO was synthesized from graphite powder employing a modified Hummers method. The morphology of synthesized composite materials was studied by scanning electron microscopy (SEM). FTIR spectroscopy analysis of PANI/rGO nanocomposites was performed using Perkin Elmer FTIR spectroscopy. Dielectric properties of nanocomposites were studied using impedance analyzer and it is observed that incorporation of rGO in PANI improves the dielectric properties. UV-VIS-NIR spectrophotometer was used to study the absorption spectra of the composite samples. The band gap energy (E_g) of the nanocomposites was determined using Tauc's relationship. It has been observed that the increasing the rGO concentration in composites reduces the optical band gap which attributes the enhancement in electron delocalization along the polymer chain. Also, the increment in protons with rGO concentration extends the density of states more into visible region of SEM spectra.

Keywords: Ultraviolet spectra, Structure of nanoscale materials, Dielectric properties of solids and liquids.

DOI: 10.21272/jnep.11(5).05026 PACS numbers: 33.20.Lg, 61.46.-W, 77.22.-d.

1. INTRODUCTION

The conducting polymers have been employed widely in diverse fields due to their synthesis simplicity, cost effectiveness, and eco-friendliness [1-2]. In conducting polymers, charge carrier transport is originated by interchain and intrachain hopping which can easily be altered by changing the configuration of polymer chain [3]. Polyaniline (PANI) is one of such materials offering high electrical to thermal conductivity ratio along with easy preparation and processibility making it useful for modern electronic components and devices [4]. PANI composites with GO and rGO also present a viable candidate for such applications among which rGO is more preferred due to its higher conductivity and thermal stability as compared to GO and therefore is being advocated as a promising material for modern electronic components and devices like supercapacitors, etc. [5].

The invention of graphene has attracted attention of researchers owing to its superior electronic, optical, mechanical and thermal properties, which can act as a building block for future electronic devices and sensors [6]. The other analogue of this family is reduced graphene oxide (rGO), which is the end result of oxidation of graphite powder and generally obtained by modified Hummer's method followed by action of a reducing agent [7].

Supercapacitor, which is also known as electric double-layer capacitor or ultracapacitor, consists of two electrodes, an electrolyte, and a separator, which isolates the two electrodes electrically as shown in Fig. 1. Supercapacitors are capable to store and transport energy with higher rates along with long life, high power, stretchy packaging, wide thermal range, low maintenance and low weight. The higher speed of charge transport is due to the charge separation mechanism at the interface between the electrode and the electrolyte [8]. Electrode material is the most important component of a supercapacitor. High-surface carbons, noble metal oxides, and conducting polymers are the main families of electrode materials being studied for supercapacitor applications [9].

Conductive polymers have been extensively studied in supercapacitors. Among conductive polymers, PANI is considered the most capable material because of its low cost, ease of synthesis and high capacitive characteristics [10]. However, the relatively poor cycling life restricts its practical applications. Recently, advancement of nanoscale binding technique provides an innovative route to prepare PANI-based nanocomposites with better performance as electrode material [11]. In the present work, PANI/rGO nanocomposite was prepared by an in-situ chemical oxidation polymerization of aniline using ammonium peroxide sulfate (APS) as an oxidizing agent.

* ajaymnit19@gmail.com

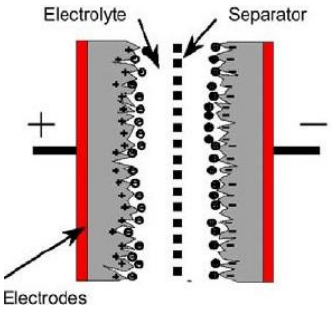

Fig 1 – Schematic representation of electrochemical double layer capacitor (EDLC)

2. EXPERIMENTAL DETAILS

The PANI/rGO composite was synthesized by an in-situ chemical oxidation polymerization of aniline using APS ($(NH_4)_2S_2O_8$) as an oxidant in presence of colloidal rGO nanoparticles at 0-5 °C in air. In a typical procedure, the rGO nanoparticles were suspended in 1 M HCl solution and sonicated for 1 h. The 0.1 M of aniline was dissolved in 100 ml of 1 M HCl solution and then mixed with 10 ml of sonicated colloidal rGO nanoparticles by further sonication for 30 min. The 100 ml of 1 M HCl solution containing the APS with an equal molar ratio to aniline was then slowly added drop-wise to well dispersed suspension mixture for 2 h with a continuous stirring at 0-5 °C. The solution was left in undisturbed position for a night for the completion of chemical reaction. The precipitate was filtered and washed with deionized water until filtered solution became neutral and then dried in vacuum for 24 h to obtain rGO/PANI composite. The different contents rGO/PANI composites were synthesized using 2, 4, 6 and 8 wt. % of rGO with respect to aniline monomer. rGO was synthesized from graphite powder employing modified Hummers method reported elsewhere [12]. The topography of specimens is investigated by scanning electron microscopy (SEM) using quanta FESEM 450 (FEI). FTIR spectrum is recorded using Perkin Elmer FTIR spectroscopy in range 4000 cm^{-1} to 500 cm^{-1}. Perkin Elmer LAMBDA 750 UV-Vis-NIR spectrophotometer is used to record absorption spectra of specimens while the dielectric properties of nanocomposites were studied using Agilent 4294A precision impedance analyzer.

3. RESULTS AND DISCUSSION

3.1 Structural Characterization

Fig. 2a displays the SEM image of pure PANI, which exhibits a relatively flat surface indicating uneven lumps in layered structure with cracks, while Fig. 2b-d show the SEM images of the composite structure. Apart from the distribution of uneven lumps and smoothed boundaries, there are not any significant changes observed from the SEM images of composites. Further, the absence of rGO structure on the surface indicates the encapsulation of rGO structure by PANI polymeric chains.

Fourier transform infrared (FTIR) spectra for pure PANI and rGO/PANI composites are shown in Fig. 3. The spectra spanned over the range 500-4000 cm^{-1} indicate similar features, which are due to the presence

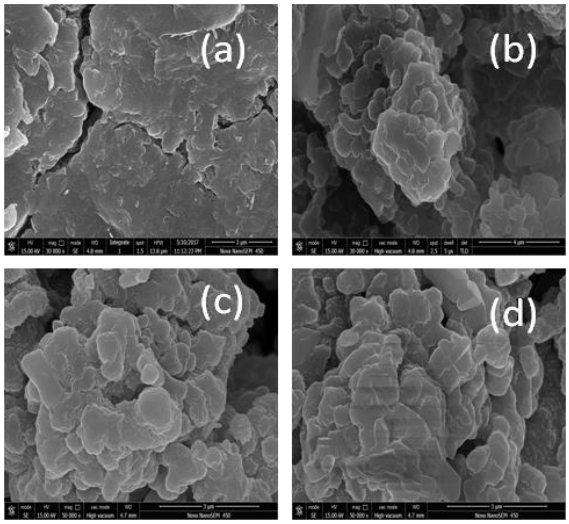

Fig. 2 – SEM images of (a) pure PANI, (b) PANI/rGO (2 %), (c) PANI/rGO (4 %), (d) PANI/rGO (8 %)

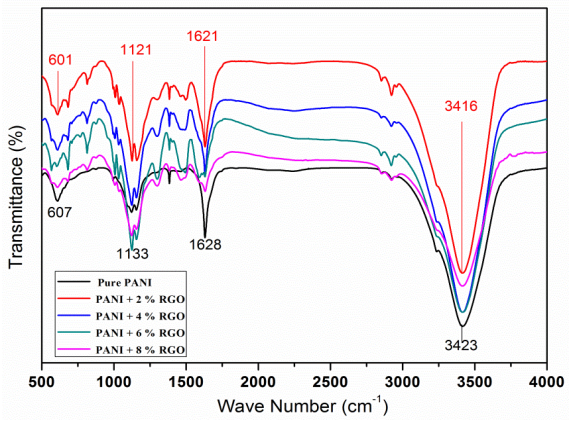

Fig. 3 – FTIR spectra of pure PANI and PANI/rGO nanocomposites

of carbonous material present in both constituents of composite material. It shows characteristic peaks at 3423, 1628, 1133 and 607 cm^{-1}, which are similar to the standard PANI reported in the literature. The major peaks at 607 and 1133 cm^{-1} for doped PANI, which is a measure of the degree of delocalization of electrons, increased for the PANI/rGO composites and are slightly shifted, which signifies an interaction between the π bonded structure of rGO and the conjugated structure of PANI. Another peak at 1628 cm^{-1} is originated due to the C=C stretching of hybridization of the sp^2 carbons of rGO [13]. Further, it is worth to mention that peaks corresponding to the characteristic group of rGO overlap with the existing peaks of PANI [11] and therefore are not marked separately.

However, a shift of wave number to a lower value is observed with the increase in concentration of rGO in the composite structure. It is expected to be due to the strong interaction between the π-bonded surfaces of rGO sheet and conjugated structure of quinoid rings of PANI [14]. Another peak at 3416 cm^{-1} is assigned to O-H stretching vibration of C-OH group. Further, it is also supported by formation of a weak charge transfer complex from aniline to rGO in which aniline acts as an electron donor, while rGO acts as an acceptor. It is also

reported to improve the electrical conductivity of composites in reports by Y. Sun, S.R. Wilson et al. [15].

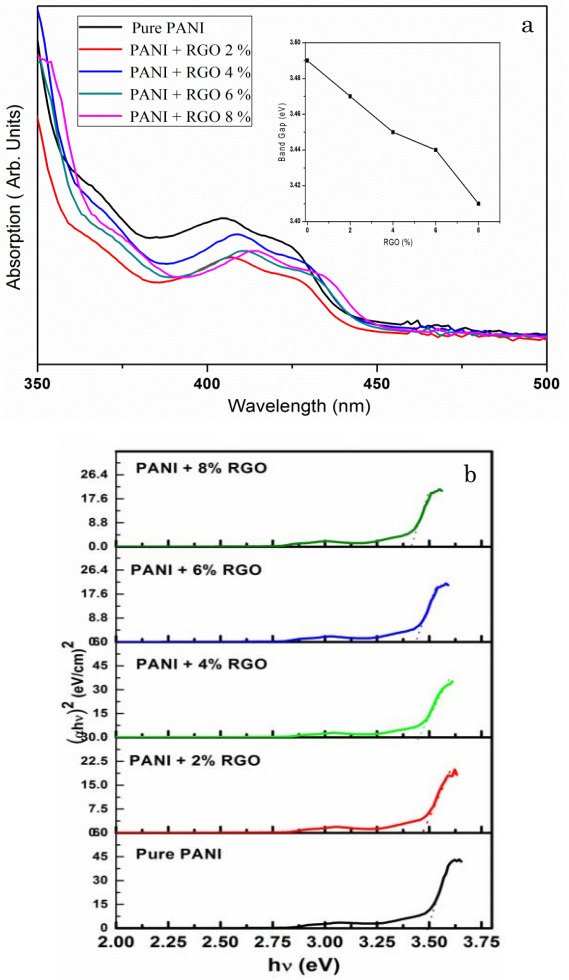

Fig. 4 – UV-Vis absorption spectrum for PANI and PANI/rGO nanocomposites (Inset shows the variation of band gap with rGo concentration) (a) and $(\alpha h\nu)^2$ versus $h\nu$ plot for PANI and PANI/rGO nanocomposites (b)

3.2 Optical Properties

The UV-Vis absorption spectra of PANI/rGO nanocomposites are as depicted in Fig. 4a. This absorption spectra curve can be attributed in four spectral regions: (i) 350-375 nm, (ii) 375-400 nm, (iii) 400-450 nm, (iv) beyond 450 nm. It is observed that the shape of spectra is quite same in all spectral regions except the variation in intensity according to wt. % of rGO nanoparticles in PANI/rGO nanocomposites. A minor band edge shift in the regions (ii) and (iii) is also observed that might be due to complex coordination among PANI molecular chain segments and encapsulated rGO nanoparticles PANI molecules [16].

The UV-Vis spectra Tauc's model is used to evaluate optical band gap (E_g) of PANI/rGO nanocomposites [12].

$$\alpha h\nu = A\left(h\nu - E_g\right)^n, \qquad (1)$$

where, h is the Planck's constant, α is the absorption coefficient, ν and A are the frequency of light and proportionality constant respectively. The value 'n' is considered 1/2 and 2 for direct and indirect transitions, respectively.

Fig. 4b depicts Tauc's plot of PANI/rGO nanocomposites. The E_g of PANI is evaluated as 3.40 eV which is in accordance to similar findings [12]. The values of E_g are found to be decreased for PANI/rGO nanocomposites up to 3.18 eV (at 8 wt. % rGO concentration) that indicates the presence of complex coordination among PANI molecular chain segments and encapsulated rGO nanoparticles PANI molecules [17].

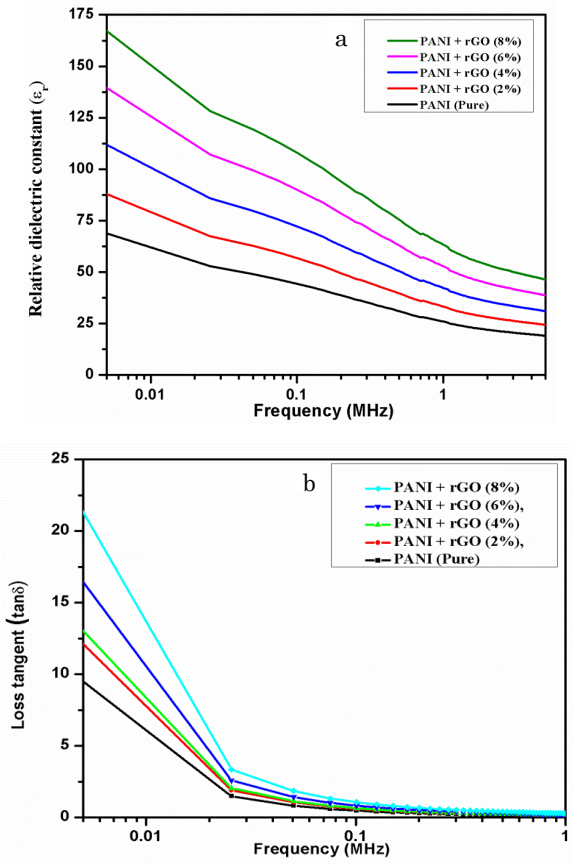

Fig. 5 – Relative dielectric constant versus frequency of PANI and PANI/rGO nanocomposites (a) and loss tangent versus frequency of PANI and PANI/rGO nanocomposites (b)

3.3 Dielectric Properties

Fig. 5 shows the variation of dielectric constant and loss tangent for PANI/rGO nanocomposites at room temperature. It is revealed that at low frequency, the dielectric constant and dielectric loss are high. On increasing frequency, these parameters decease stridently and become almost constant at higher frequencies depicting the predictable diffusion that can be attributed through Debye-like relaxation mechanism [18]. In accordance to this, at lower frequency region, dipole moment of rGO encapsulated PANI molecules tags along the applied field that enhances dielectric constant, whereas with the increase in the frequency, the applied field unable to induce such dipole moment that further causes decrement in dielectric constant accordingly [19, 20].

From the results described above, it has been considered that the enhanced dielectric constants and

losses might originate from the increased conductivity. The increased conductivity is attributed to the formation of a better charge transport network in the relatively polyaniline matrix. The dielectric performance of the PANI/rGO composites was enhanced compared with that of either PANI or rGO alone.

4. CONCLUSIONS

In the light of above efficient investigations, the following conclusions are drawn:

(1) Pure PANI and PANI/rGO nanocomposites are structurally confirmed through SEM and FTIR observations. SEM image of pure PANI shows the relatively flat surface indicating uneven lumps in layered structure with cracks. Apart from the distribution of uneven lumps and smoothed boundaries, there are not any significant changes observed from the SEM images of composites.

(2) FTIR study reveals that all PANI/rGO nanocomposites exhibit the main characteristic peaks almost at 3423, 1628, 1133 and 607 cm^{-1} corresponding to different stretching modes of PANI, and peak at 1628 cm^{-1} originates due to the C=C stretching of hybridization of the sp^2 carbons of rGO.

(3) The optical study of PANI/rGO nanocomposites is revealed through the UV-Vis absorption spectra within 350 to 500 nm. Their respective Tauc plots indicate that the value of E_g of pure PANI enhances from 3.40 eV to 3.18 eV with raise in the rGO wt. % concentration in the PANI/rGO nanocomposites.

(4) Dielectric analysis reveals that the PANI/rGO nanocomposites offer higher dielectric constant and dielectric loss at low frequency. The dielectric performance of the PANI/rGO composites was enhanced compared with that of either PANI or rGO alone.

REFERENCES

1. Y. Hu, H. Shi, H. Song, C. Liu, J. Xu, L. Zhang, Q. Jiang, *Synthetic Metals* **181**, 23 (2013).
2. H. Park, S.H. Lee, F.S. Kim, H.H. Choi, I.W. Cheong, J.H. Kim, *J. Mater. Chem. A* **2** No 18, 6532 (2014).
3. Y. Long, Z. Chen, X. Zhang, J. Zhang, Z. Liu, *Appl. Phys. Lett.* **85** No 10, 1796 (2004).
4. A.K. Sharma, R. Vyas, P.K. Jain, U. Chand, V.K. Jain, *J. Nano-Electron. Phys.* **11** No 2, 02012 (2019).
5. L.F. Miranda, P.V.C. Gomes, F.J.M. Almeida, G.A. e Silva, A.H.M. Junior, T.J. Masson, *In Characterization of Minerals, Metals, and Materials*, 773 (Springer: Cham.: 2019).
6. X. Tian, S. Sarkar, A. Pekker, M.L. Moser, I. Kalinina, E. Bekyarova, R.C. Haddon, *Carbon* **72**, 82 (2014).
7. M. Mitra, K. Chatterjee, K. Kargupta, S. Ganguly, D. Banerjee, *Diam. Relat. Mater.* **37**, 74 (2013).
8. H.P. Wu, D.W. He, Y.S. Wang, M. Fu, Z.L. Liu, J.G. Wang, H.T. Wang, *2010 8th International Vacuum Electron Sources Conference and Nanocarbon*, 465 (IEEE: 2010).
9. Z.S. Iro, C. Subramani, S.S. Dash, *Int. J. Electrochem. Sci.* **11** No 12, 10628 (2016).
10. S. Srivastava, S.S. Sharma, S. Kumar, S. Agrawal, M. Singh, Y.K. Vijay, *Int. J. Hydrogen Energy* **34** No 19, 8444 (2009).
11. R. Kumar, T. Bhuvana, G. Mishra, A. Sharma, *RSC Adv.* **6** No 77, 73496 (2016).
12. M. Mitra, C. Kulsi, K. Chatterjee, K. Kargupta, S. Ganguly, D. Banerjee, S. Goswami, *RSC Adv.* **5** No 39, 31039 (2015).
13. Y. Li, Y. Zheng, *J. Appl. Polymer Sci.* **135** No 16, 46103 (2018).
14. S. Quillard, G. Louarn, S. Lefrant, A.G. MacDiarmid, *Phys. Rev. B* **50** No 17, 12496 (1994).
15. Y. Sun, S.R. Wilson, D.I. Schuster, *J. Amer. Chem. Soc.* **123** No 22, 5348 (2001).
16. Y. Du, K.F. Cai, S.Z. Shen, P.S. Casey, *Synth. Met.* **162** No 23, 2102 (2012).
17. X. Li, G. Wang, X. Li, D. Lu, *Appl. Surf. Sci*, **229** No 1-4, 395 (2004).
18. Ajay Kumar Sharma, Praveen Kumar Jain, Rishi Vyas, Vipin Kumar Jain, *Asian J. Chem.* **31**, 855 (2019).
19. N. Sharma, V. Sharma, S.K. Sharma, K. Sachdev, *Mater. Lett.* **236**, 444 (2019).
20. J. Xiang, L.T. Drzal, *Polymer* **53** No 19, 4202 (2012).

Покращені оптичні та діелектричні властивості нанокомпозитів PANI/rGO для застосування в суперконденсаторах

Ajay Kumar Sharma[1,2], Praveen Kumar Jain[3], Rishi Vyas[2], Vishal Mathur[4], Vipin Kumar Jain[1]

[1] *Institute of Engineering and Technology, JK Lakshmipat University, Jaipur 302026, India*
[2] *Department of Physics, Swami Keshvanand Institute of Technology, Management & Gramothan, Jaipur 302017, India*
[3] *Department of Electronics and Communication Engineering, Swami Keshvanand Institute of Technology, Management & Gramothan, Jaipur 302017, India*
[4] *Department of Engineering, Sur University College, Oman*

Провідні полімерні нанокомпозити широко використовуються завдяки різноманітним застосуванням, зокрема, як новітній суперконденсатор. Робота стосується виготовлення нанокомпозитів PANI/rGO та дослідження їх морфологічних, оптичних та діелектричних властивостей. Робота зосереджена на синтезі нанокомпозитів $(PANI)_{1-x}(rGO)_x$ (x = 0, 0.02, 0.04, 0.06, 0.08), виготовлених методом хімічної окислювальної полімеризації аніліну in-situ з використанням пероксидисульфату амонію (APS) як окислювача у присутності наночастинок колоїдного зменшеного оксиду графену (rGO) при температурі 0-5 °C для поліпшення оптичних і діелектричних констант PANI для застосування в суперконденсаторах. rGO синтезувався з графітового порошку, використовуючи модифікований метод Хаммерса. Морфологію синтезованих композиційних матеріалів вивчали за допомогою скануючої електронної мікроскопії (SEM). Аналіз спектроскопії FTIR нанокомпозитів PANI/rGO проводили за допомогою спектроскопії Perkin Elmer FTIR. Діелектричні властивості нанокомпозитів вивчалися за допомогою аналізатора імпедансу, і спостерігається, що включення rGO в PANI покращує діелектри-

чні властивості. Для дослідження спектрів поглинання композиційних зразків використовували спектрофотометр ультрафіолетового випромінювання UV-VIS-NIR. Енергія забороненої зони (E_g) нанокомпозитів визначалася за відношенням Таука. Було помічено, що підвищення концентрації rGO в композитах зменшує оптичну ширину забороненої зони, що пояснює посилення делокалізації електронів уздовж полімерного ланцюга. Також приріст протонів з ростом концентрації rGO розтягує діапазон щільності станів більше у видиму область SEM-спектрів.

Ключові слова: Ультрафіолетовий спектр, Структура нанорозмірних матеріалів, Діелектричні властивості твердих тіл і рідин.